*11352–11362* *Nucleic Acids Research, 2012, Vol. 40, No. 22* *Published online 18 October 2012*
*doi:10.1093/nar/gks973*

# RNA polymerase-promoter interactions determining different stability of the *Escherichia coli* and *Thermus aquaticus* transcription initiation complexes

**Vladimir Mekler[1,*], Leonid Minakhin[1], Konstantin Kuznedelov[1], Damir Mukhamedyarov[1] and Konstantin Severinov[1,2,3,*]**

[1]Waksman Institute of Microbiology and [2]Department of Molecular Biology and Biochemistry, Rutgers, State University of New Jersey, Piscataway, NJ 08854, USA and [3]Institutes of Molecular Genetics and Gene Biology, Russian Academy of Sciences, Moscow 119334, Russia

Received July 23, 2012; Revised September 18, 2012; Accepted September 25, 2012

## ABSTRACT

**Transcription initiation complexes formed by bacterial RNA polymerases (RNAPs) exhibit dramatic species-specific differences in stability, leading to different strategies of transcription regulation. The molecular basis for this diversity is unclear. Promoter complexes formed by RNAP from *Thermus aquaticus* (*Taq*) are considerably less stable than *Escherichia coli* RNAP promoter complexes, particularly at temperatures below 37°C. Here, we used a fluorometric RNAP molecular beacon assay to discern partial RNAP-promoter interactions. We quantitatively compared the strength of *E. coli* and *Taq* RNAPs partial interactions with the −10, −35 and UP promoter elements; the TG motif of the extended −10 element; the discriminator and the downstream duplex promoter segments. We found that compared with *Taq* RNAP, *E. coli* RNAP has much higher affinity only to the UP element and the downstream promoter duplex. This result indicates that the difference in stability between *E. coli* and *Taq* promoter complexes is mainly determined by the differential strength of core RNAP–DNA contacts. We suggest that the relative weakness of *Taq* RNAP interactions with DNA downstream of the transcription start point is the major reason of low stability and temperature sensitivity of promoter complexes formed by this enzyme.**

## INTRODUCTION

Transcription is the first step of gene expression and a target of extensive regulation. The bacterial DNA-dependent RNA polymerase (RNAP) is the principal enzyme of transcription. The bacterial RNAP initiates transcription in the form of the holoenzyme (subunit composition $\alpha I \alpha II \beta \beta' \omega \sigma$). The dissociable specificity subunit $\sigma$ is required for promoter recognition and melting (1,2). Bacterial genomes encode multiple $\sigma$ factors, each targeting RNAP core to a particular group of promoters with common sequence (3). One $\sigma$, called primary, is usually present at the highest amounts and enables RNAP to recognize the majority of promoters required for expression of genes under normal physiological conditions.

Despite the functional and sequence similarities between the primary $\sigma$ subunits from various bacteria, promoter complexes formed by corresponding holoenzymes exhibit dramatic species-specific differences in their stability and efficiency of transition from initiation to elongation stages of transcription. These differences have been clearly revealed in the context of model enzymes of bacterial transcription—RNAPs from *Escherichia coli*, *Bacillus subtilis* and two closely related thermophilic bacteria, *Thermus aquaticus* (*Taq*) and *Thermus thermophilus* (*Tth*). These holoenzymes recognize the same conserved promoter elements centered around −10 and −35 positions (consensus sequences are TATAAT and TTGACA, respectively). *B. subtilis* RNAP forms unstable open complexes ($RP_o$) at the majority of promoters. These complexes are in equilibrium with closed complexes and, in turn, with free RNAP (4). To provide the energy required to stimulate $RP_o$ formation, thermophilic bacteria depend on the high

*To whom correspondence should be addressed. Tel: +848 445 6095; Fax: +848 445 5735; Email: mekler@waksman.rutgers.edu
Correspondence may also be addressed to Konstantin Severinov. Tel: +848 445 6096; Fax: +848 445 5735; Email: severik@waksman.rutgers.edu

temperatures of their environment. Holoenzymes from *Taq* (*Taq* $E\sigma^A$), *Tth* and other related thermophilic bacteria form moderately stable open complexes at ~60°C. These complexes become very unstable at temperatures below 37°C (5–11). In contrast, open complexes formed by *E. coli* RNAP holoenzyme (*Ec* $E\sigma^{70}$) at many promoters are stable even at physiologically suboptimal temperatures (20–25°C), and, in many cases, the $RP_o$ formation is essentially irreversible (2). However, at some promoters, *Ec* $E\sigma^{70}$ does form intrinsically unstable open complexes, with *E. coli rrnB* P1 promoter being the best-studied model. Stability of the *rrnB* P1 open complex is a subject of genetic regulation and is determined by concentration of the initiating NTP and by ppGpp and DksA (12). Efficient transcription from promoters with unstable open complexes is often observed and could be caused by facilitated promoter escape, which should increase the rate of transition from transcription initiation to transcription elongation. Indeed, *B. subtilis* and *Taq* RNAPs are less prone to abortive RNA synthesis than the *E. coli* enzyme during transition to elongation from the same promoters (4,9,11). The pronounced differences in RNAPs behavior during initiation and transition to elongation steps may result in different strategies of control of the transcription process (4,13).

Species-specific variations of strength of RNAP interactions with certain promoter segments can account for overall differences in promoter complex properties, including their stability and temperature sensitivity. In principle, promoter contacts with RNAP core, σ or both can be responsible for these differences. Schroeder and deHaseth (10) found that oligonucleotides and upstream fork junction promoter fragments containing the consensus −10 and −35 element sequences bound to *Taq* RNAP similarly or even stronger than to *E. coli* RNAP, as judged by sensitivity of the RNAP–DNA probe complexes to heparin. This result suggests that the strengths of *Taq* and *E. coli* RNAPs interactions with the basal promoter elements may not correlate with efficiencies of the $RP_o$ formation by these enzymes. In contrast to the *E. coli* RNAP, no sequence-specific interaction of *Thermus* RNAP α subunits with promoter UP element was found (14). However, as the upstream promoter interactions are necessary for the initiation complex formation only at a fraction of *Ec* $E\sigma^{70}$ promoters, the difference in strength of these interactions can not solely explain the generally higher stability of *Ec* $E\sigma^{70}$ promoter complexes. Several studies suggested that many differences between bacterial transcription complexes can be due to the changes in contacts made between the downstream DNA duplex and the core RNAP β and β′ subunits (4,15–17). Miropolskaya *et al* (11) recently showed that the structures of the N-terminal regions 1.1 and 1.2 of the *E. coli* $\sigma^{70}$ and *Taq* $\sigma^A$ subunits in part determine higher stability of *E. coli* RNAP promoter complexes. It seems plausible that the effect of σ region 1.1 on promoter complex stability is also related with modulating strength of RNAP interactions with the downstream promoter duplex (11). However, direct data on comparative strengths of downstream contacts for RNAPs from different bacteria are currently unavailable. Thus, although the species-specific peculiarities of $RP_o$ formation in bacteria are well established, the molecular basis for this diversity is unclear.

A recently reported *E. coli* RNAP beacon assay (18) was previously used to measure specific affinity of *Ec* $E\sigma^{70}$ to various model promoter fragments and quantitatively characterize partial *E. coli* RNAP promoter interactions (18–21). Here, we developed a similar beacon assay for *Taq* $E\sigma^A$. This approach allowed us to comprehensively compare the strengths of partial RNAP-promoter interactions that are known to be essential for $RP_o$ formation by *Ec* $E\sigma^{70}$ and *Taq* $E\sigma^A$. The data form a basis for quantitative rationalization of a number of previously described biochemical observations. In particular, we found that in the context of RNAP complexes with model promoter fragments, *Taq* $E\sigma^A$ interacts with the downstream promoter duplex much weaker than does *Ec* $E\sigma^{70}$. This result provides direct quantitative evidence that the strength of downstream RNAP-promoter contacts varies considerably in different bacteria and can therefore be an important factor determining species-specific stability and, by extension, modes of regulation of promoter complexes.

## MATERIALS AND METHODS

### Proteins

Expression plasmids pET28Taq$\sigma^A$ and pET28Tth$\sigma^A$ encoding *T. aquaticus* and *T. thermophilus* $\sigma^A$ subunits, respectively, were used for site-specific mutagenesis and subsequent purification of polyhistidine-tagged mutant protein derivatives with single Cys residues. *Taq* core RNAP, wild-type and Cys $\sigma^A$ derivatives were purified as described in (8). The recombinant system used for the preparation of *Taq* RNAP yields highly active enzyme that is indistinguishable from the 'native' enzyme purified from *Taq* cell cultures in biochemical assays (8,22). *Tth* RNAP and Cys $\sigma^A$ derivatives were purified as described in (23). Fluorescent labels were incorporated into single-Cys $\sigma^{70}$ and $\sigma^A$ derivatives using Cys-specific chemical modification [procedures as described in (24), efficiencies of labeling were >70%]. RNAP holoenzymes containing the labeled σ derivatives were prepared as in (24).

### DNA probes

DNA oligonucleotides were synthesized by Integrated DNA Technologies. Fork junction and double-stranded DNA probes were prepared as in (18).

### Fluorometric assays

Fluorescence measurements were performed using a QuantaMaster QM4 spectrofluorometer (PTI) in transcription buffer [40 mM Tris–HCl (pH 8.0), 100 mM NaCl, 5% glycerol, 1 mM DTT and 10 mM $MgCl^2$] containing 0.02% Tween 20 at 25 or 45°C. Final assay mixtures (800 μl) contained 1 nM labeled RNAP holoenzyme and DNA probes at various concentrations. The Tetramethylrhodamine-5-maleimide (TMR) fluorescence intensities were recorded with an excitation wavelength of 550 nm and an emission wavelength of 578 nm.

To obtain equilibrium dissociation constants ($K_d$), the experimental dependence of the fluorescent signal amplitude (F) on DNA probe concentration was fit to Equation 1, unless otherwise noted.

$$(1 - X)([DNA] - [RNAP]X) = K_dX \quad (1)$$

where $X = (F\text{-}F_0)/(F_{max}\text{-}F_o)$, $F_o$ is the initial value of the amplitude, and $F_{max}$ is the limiting value of the amplitude at $[DNA] = \infty$. The data were analysed using SigmaPlot software (SPSS, Inc.).

To prevent dissociation of relatively short duplexes in downstream fork junctions, in particular at 45°C, 100 nM excesses of template strand fragments of these probes were added to the assayed samples. Control experiments verified that the template strand oligos generated negligibly low signals and did not interfere with binding of the downstream fork junctions.

An equilibrium competition binding assay was used to measure affinity of tight *E. coli* RNAP complexes with fork junction probes 8, 12 and 13 (Figure 2 and Supplementary Figure S2). A double-stranded [−58/−14] fragment of N25cons producing negligible signal on binding to (211Cys-TMR) $\sigma^{70}$ holo RNAP was used as a competitor, as described in (18). Time-dependent fluorescence changes were monitored after manual-mixing of RNAP beacon (800 µl) and a DNA probe (<20 µl) in a cuvette; the mixing dead-time was 15 s.

### *In vitro* abortive initiation assay

Abortive transcription reactions were performed in a final volume of 10 µl and contained 200 nM *Ec* E$\sigma^{70}$ (Epicentre) or *Taq* E$\sigma^{A}$, and 50 nM N25cons promoter DNA in transcription buffer [30 mM Tris–HCl (pH 7.9), 40 mM KCl, 10 mM $MgCl_2$, 2 mM β-mercaptoethanol]. Reactions were mixed and incubated for 10 min at optimal temperatures 37°C (for *E. coli* RNAP) or at 55°C (for *Taq* RNAP) followed by 5 min incubation with 50 µg/ml heparin or 0.5 µM of fork junction DNA competitor (where indicated). Next, the reactions were incubated for a further 10 min at optimal 37°C or 55°C with added transcription hot mix [200 µM CpA RNA dinucleotide primer, 20 µM cold UTP, and ($\alpha$-$^{32}$P)UTP (3000 Ci/mmol)] and then terminated with an equal volume of urea-formamide loading buffer. Alternatively, the reaction mixtures after incubation at the optimal temperatures were placed at suboptimal temperature 25°C, supplemented with heparin (where indicated) and incubated for a further 10 min with transcription hot mix at the same temperature. The reaction products were resolved on a 20% (w/v) polyacrylamide denaturing gel and visualized using a PhosphorImager. Abortive initiation experiments were repeated two or three times, with standard deviation ≤20%.

## RESULTS

### Development of a protein beacon assay to study the interactions of thermophilic RNAPs with promoters

A recently developed RNAP molecular beacon assay allows one to monitor the *Ec* E$\sigma^{70}$ interactions with promoters and a wide variety of model DNA substrates mimicking DNA structures in the open promoter complex (18). The assay relies on the detection of fluorescence signal from RNAP holoenzyme containing the $\sigma^{70}$ subunit with fluorescent label site-specifically incorporated in proximity to region 2.3, the part of σ that recognizes the −10 promoter element. The base-line fluorescence of labeled RNAP holoenzyme is low owing to quenching by $\sigma^{70}$ region 2 Trp and Tyr residues via photoinduced electron transfer mechanism. Efficient quenching usually occurs at length scales below 1 nm. On RNAP interaction with promoter DNA or promoter fragments, the aromatic amino acids lose contact with the fluorescent probe, decreasing the quenching efficiency leading to increased fluorescence.

In this work, we developed new RNAP beacons based on RNAPs from two bacteria of the *Thermus* genus, *T. aquaticus* and *T. thermophilus*. *Taq* E$\sigma^{A}$ beacons were developed similarly to the previously described *Ec* E$\sigma^{70}$ beacons (18). Single-cysteine mutants of the *Taq* RNAP $\sigma^{A}$ subunit that allow site-specific introduction of fluorescent labels were prepared. The sites where unique cysteine residues were introduced (aminoacid positions 243 and 245) were chosen, based on available structures of *Taq* $\sigma^{A}$ domain 2 (21,25). Fluorescent labels attached to cysteines at these positions should be close to Trp residues of $\sigma^{A}$ region 2.3. Therefore, these Trp residues may quench the fluorescence of site-specifically attached fluorophores. The positions of $Cys^{243}$ and $Cys^{245}$ on a structural model of the $\sigma^{A}$–DNA complex (21) are shown in Figure 1. As can be seen, the bases of the −10 element, in particular the -11A base, are located just between the modified SH groups and the $Trp^{256}$/$Trp^{257}$ side chains, suggesting that specific binding to promoter should unquench the signal from the fluorescent label.

To determine whether $\sigma^{A}$-based beacons function as expected, single-cysteine $\sigma^{A}$ mutants were modified with TMR (the efficiency of labeling was at least 80%) and used to reconstitute *Taq* RNAP holoenzyme. Both mutant holoenzymes were functional (at least 70% of the wild-type *Taq* E$\sigma^{A}$ activity in abortive initiation assay on the *galP1* promoter, data not shown). When E$\sigma^{A}$ holoenzymes containing fluorescent labels at $\sigma^{A}$ positions 243 and 245 were combined with DNA fragments containing the T5 N25 promoter (Figure 2), the fluorescence signal increased ~1.7 and 2.3-fold, respectively. A similar result was obtained with other promoters (N25cons and *gal*P1). Data presented below show that increased fluorescence was owing to specific RNAP interaction with the −10 promoter element, allowing us to conclude that *Taq* $\sigma^{A}$-based beacons function as expected.

We also tested a number of similarly purified and labeled *Tth* $\sigma^{A}$ derivatives. The *Tth* RNAP holoenzyme containing $\sigma^{A}$ with TMR attached at 230 position demonstrated readily measurable 'beacon effect' similar to those observed with the *Taq* RNAP beacons.

In what follows, we use the *Taq* E$\sigma^{A}$ beacon based on (245Cys-TMR)$\sigma^{A}$ and a previously described *Ec* E$\sigma^{70}$ beacon (18) based on (211Cys-TMR)$\sigma^{70}$ to quantitatively compare RNAP affinities to various promoter fragments. Dissociation constants ($K_d$) measured by the *E. coli*

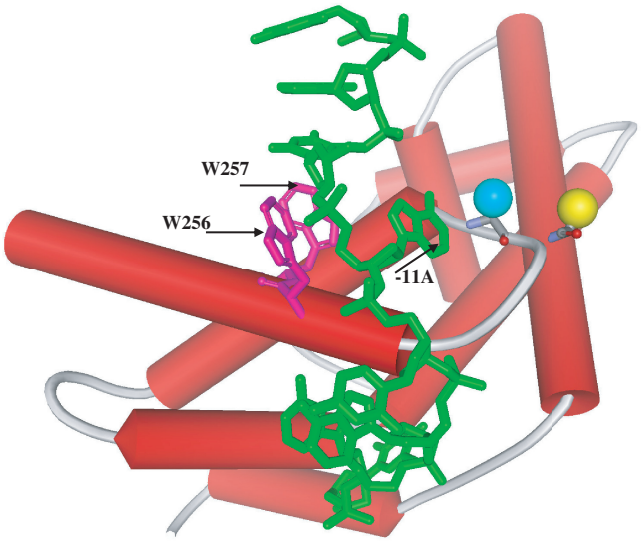


**Figure 1.** Structural model of $\sigma^A$ domain 2 bound to single-stranded DNA (in green) showing the positions of SH groups in single-cystein $\sigma^A$ derivatives 245Cys (yellow sphere) and 243Cys (blue sphere). The structure is from (21).

RNAP beacon assay were slightly higher than $K_d$ values measured using other methods, presumably because in the beacon assay, some binding free energy must be used to disrupt the van der Waals contacts between the fluorophore and the quenching aromatic amino acids (18). The strengths of the fluorophore-quencher contacts may be not equal in the *Taq* $E\sigma^A$ and *Ec* $E\sigma^{70}$ beacons, though the use of the same fluorescent label in the both beacons should help diminish the difference. Be that as it may, this effect could somewhat affect comparison of the *Taq* $E\sigma^A$ and *Ec* $E\sigma^{70}$ beacon interactions with the −10 element *per se* and immediately adjacent bases, but it should not influence the RNAP affinities to promoter parts that are remote from the −10 element.

## DNA probes

Certain promoter fragments are known to interact with RNAP, and resulting complexes mimic RNAP interactions with corresponding promoter segments in complexes with full-sized promoters. These model substrates include DNA oligos containing sequences corresponding to the non-template strand of the −10 promoter element (26), upstream fork junctions (27–29), downstream fork junctions (19) and short double-stranded promoter fragments (19,21). Studies of RNAP interactions with such fragments can be used to dissect partial RNAP-promoter interactions. The RNAP beacon assay is well-suited for this purpose owing to its high sensitivity and low intensity of non-specific background signal.

We compared the strength of interactions of *Taq* $E\sigma^A$ and *Ec* $E\sigma^{70}$ with model promoter fragments schematically shown in Figure 2. Together, these DNA probes encompass the entire promoter length and include all essential promoter elements. The DNA probes are based on T5 N25 and N25cons promoter sequences (Figure 2). N25cons is a 'full consensus' derivative of T5 N25 with consensus −35 element, an optimized UP element, and the extended −10 element (20). For *E. coli* RNAP, the strength of interactions with many of the probes shown in Figure 2 was measured previously using the beacon assay (18–20).

*Taq* $E\sigma^A$ is highly active on N25cons in the abortive transcription initiation assay at 55°C. The activity is reduced ~10-fold when an open complex formed at 55°C is shifted to 25°C and then supplemented with abortive transcription reaction substrates (Figure 3). To evaluate *Taq* $E\sigma^A$-N25cons complex stability, we measured activity of preformed complex after a 5-min incubation with 50-μg/ml heparin, which is known to compete with DNA for the binding to RNAP. As shown in Figure 3, *Taq* $E\sigma^A$-N25cons complex was very unstable at 25°C: heparin treatment resulted in a 14-fold drop in activity. Heparin sensitivity at 55°C was less pronounced (1.7-fold drop in activity, Figure 3). In contrast, the activity of preformed *Ec* $E\sigma^{70}$-N25cons complex decreased only slightly (by ~15%) after incubation with heparin at either 25°C or 37°C (Figure 3). In principle, *Taq* $E\sigma^A$ and *Ec* $E\sigma^{70}$ may bind heparin with different strength, which could modulate the relationship between promoter stabilities and heparin sensitivities. Therefore, we compared stabilities of *Taq* $E\sigma^A$ and *Ec* $E\sigma^{70}$ complexes with T5 N25 and N25cons promoter DNA fragments at 55°C and 37°C, respectively, using a fork junction fragment of N25cons (shown in Supplementary Figure S1A), rather than heparin, as a competitor. The fork junction competitor formed very tight and inactive complexes with both *Taq* and *Ec* enzymes (data not shown). In agreement with the result obtained with heparin, we found that activities of the *Taq* $E\sigma^A$ promoter complexes decreased considerably faster in the presence of the fork junction competitor than activities of *Ec* $E\sigma^{70}$ promoter complexes (Supplementary Figure S1B).

Thus, promoter complexes formed by *Taq* and *E. coli* RNAPs on N25cons and T5N25 demonstrate differences in stability that are consistent with results obtained previously on other promoters (6–11).

The affinities of DNA probes to *Taq* $E\sigma^A$ and *Ec* $E\sigma^{70}$ beacons were characterized by determining dissociation constants values and are listed in Tables 1 and 2. Most of the measurements were carried out at 25°C; some experiments with *Taq* $E\sigma^A$ were also performed at 45°C. Representative experimental data for *Taq* $E\sigma^A$ are shown in Figure 4.

## Interactions of *Taq* $E\sigma^A$ and *Ec* $E\sigma^{70}$ with oligos containing the −10 promoter element sequence

As a starting point, we compared *Taq* $E\sigma^A$ and *Ec* $E\sigma^{70}$ affinities with an oligonucleotide corresponding to non-transcribed strand positions −12/+2 of the T5 N25 promoter (probe 1). A mutant oligo 2 with a T for C substitution at a highly conserved position −7 was used as control. The −12/+2 oligo bound *Taq* $E\sigma^A$ RNAP about 2-fold better than *Ec* $E\sigma^{70}$ ($K_d$ = 100 and 160 nM, respectively). The same ratio of affinities was found for the


**Figure 2.** Structures of DNA probes used. The probe names used in the text are in red. In fork junction probe names, numbers in left and right parentheses correspond to borders of upper and bottom strands of fork junctions with respect to the transcription start located at +1 (underlined). The −10 and −35 promoter element sequences are highlighted in larger size font. Asterisks above the [−40/+20] probe indicate positions where the fragments used in experiment shown in Figure 5 were truncated.

shorter −12/−6 probe 5. The control, −12/+2;−7C oligo, bound *Taq* Eσ$^A$ poorly (Figure 4A), testifying that *Taq* σ$^A$-based beacon is specific. The GGGA motif located immediately downstream of the −10 promoter element contributes to the strength of promoters recognized by *Taq* σ$^A$ RNAP and is likely recognized by region 1.2 of σ (30,31). We measured the effect of substitution of the −12/+2 oligo positions −6/−3 (AGAT) for the optimal sequence GGGA (probe 3) and unfavorable sequence CCCT (probe 4) on RNAP binding. The substitutions caused considerable, ∼100-fold, change in affinity to *Taq* Eσ$^A$, whereas only ∼10-fold change was observed with *Ec* Eσ$^{70}$ (Figure 4A, Table 1). These data correlate well with reported effects caused by similar sequence changes on efficiencies of transcription initiation by these enzymes, suggesting that the downstream promoter motif is more important for *Taq* RNAP than for *E. coli* RNAP (32).

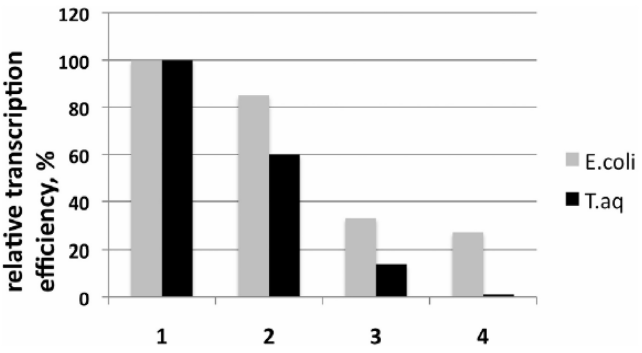


**Figure 3.** Stabilities of transcription initiation complexes of *T. aquaticus and E. coli* RNAPs. The plot shows relative efficiencies of abortive transcription initiation reactions by *E. coli* and *T. aquaticus* RNAP holoenzymes at N25cons promoter DNA fragment. All samples were initially incubated for 10 min at optimal (37°C for *E. coli* and 55°C for *T. aquaticus*) temperatures. Next, four reactions (1–4) were carried out as following: at the optimal temperatures, either immediately after the initial incubation (1) or after 5 min additional incubation with 50 μg/ml heparin (2). After the initial incubation, samples 3 and 4 were further incubated at 25°C for 15 min, followed by the reactions either without (3) or after the heparin treatment (4).

## Interactions of Taq Eσ$^A$ and Ec Eσ$^{70}$ with upstream fork junctions

To compare *Taq* Eσ$^A$ and *Ec* Eσ$^{70}$ interactions with the part of promoter located upstream of the −10 element, we measured the affinities of several upstream fork junctions (probes 6–13). The measurements could not be carried out using probes with identical single-stranded fragments because $K_d$ values for probes with the shortest and longest double-stranded segments differed by $>10^5$-fold, making quantitaive analysis technically impossible in some cases. To circumvent this problem, probe affinities were adjusted by changing the length of the single-stranded segment. Probe 11, bearing the shortest duplex segment with upstream end at position −26, bound *Taq* Eσ$^A$ and *Ec* Eσ$^{70}$ with similar affinities ($K_d$ = 0.65 and 0.46 nM, respectively). Other upstream forks contained longer double-stranded segments. One series of probes extended to position −38 and allowed to evaluate the contribution of the −35 promoter element to RNAP-promoter interaction. *Ec* Eσ$^{70}$ bound probes 6–8 (contain consensus −35 element sequence) 3- to 6-fold stronger than *Taq* Eσ$^A$. Conversely, we found that probe 10 bearing a mutated −35 element had ∼4-fold higher affinity to *Taq* Eσ$^A$ than to *Ec* Eσ$^{70}$. The result suggests that *Taq* Eσ$^A$ may have higher affinity to non-consensus −35 element bases than *Ec* Eσ$^{70}$.

The structures of probes 6 and 7 are identical, except for the TG extended −10 promoter motif present in probe 7 (positions −14/−15). The respective $K_d$ values of *Taq* Eσ$^A$ and *Ec* Eσ$^{70}$ binding to probe 6 are 12-fold higher than to probe 7 (Table 1). Thus, the contribution of TG to the binding of both enzymes is equal.

On the whole, the data obtained with probes extending up to position −38 suggest that although the modes of *Taq* Eσ$^A$ and *Ec* Eσ$^{70}$ interactions with the −35 element may be somewhat different, the overall difference of interaction with the −10 and −35 promoter elements between Eσ$^A$ and Eσ$^{70}$ is not very large and is therefore unlikely to account for observed large differences in stabilities of promoter complexes formed by these enzymes.

**Table 1.** Dissociation constants for the binding of promoter fragments to *Taq* Eσ$^A$ and *Ec* Eσ$^{70}$ at 25°C

| Promoter fragments | DNA probe | $K_d^{taq}$, nM | $K_d^{ec}$, nM | $K_d^{taq}/K_d^{ec}$ |
|---|---|---|---|---|
| Oligos | 1. −12/+2 | 100 | 160 | 0.63 |
| | 3. −12/+2; ggga | 15 | 110 | 0.14 |
| | 4. −12/+2; ccct | 2200 | 690 | 3.2 |
| | 5. −12/−6 | 54000 | 80000 | 0.68 |
| Upstream fork junctions | 6. [−38/−11][−38/−12] | 13.7 | 5 | 2.8 |
| | 7. [−38/−11][−38/−12]TG | 1.2 | 0.43 | 2.8 |
| | 8. [−38/−8][−38/−12] | 0.8 | 0.14 | 5.7 |
| | 9. [−38/−7][−38/−12] | <0.2 | <0.2 | |
| | 10. [−38/−7][−38/−12] −35mut | 0.57 | 2.1 | 0.27 |
| | 11. [−26/−3][−26/−12] | 0.65 | 0.46 | 1.4 |
| | 12. [−59/−11][−59/−12]UP*ec* | 4.1 | 0.008 | 510 |
| | 13. [−59/−11][−59/−12]UP*th* | 3.4 | 0.35 | 9.7 |
| Downstream fork junctions | 14. [−12/+20][+3/+20] | 1.6 | <0.2 | >8 |
| | 15. [−12/+20][+3/+20]ggga | 0.2 | <0.2 | |
| | 16. [−11/+14][+2/+14] | 42 | 0.25 | 170 |

The $K_d$ values presented are averages obtained from two to three individual experiments, the error is ±15%.

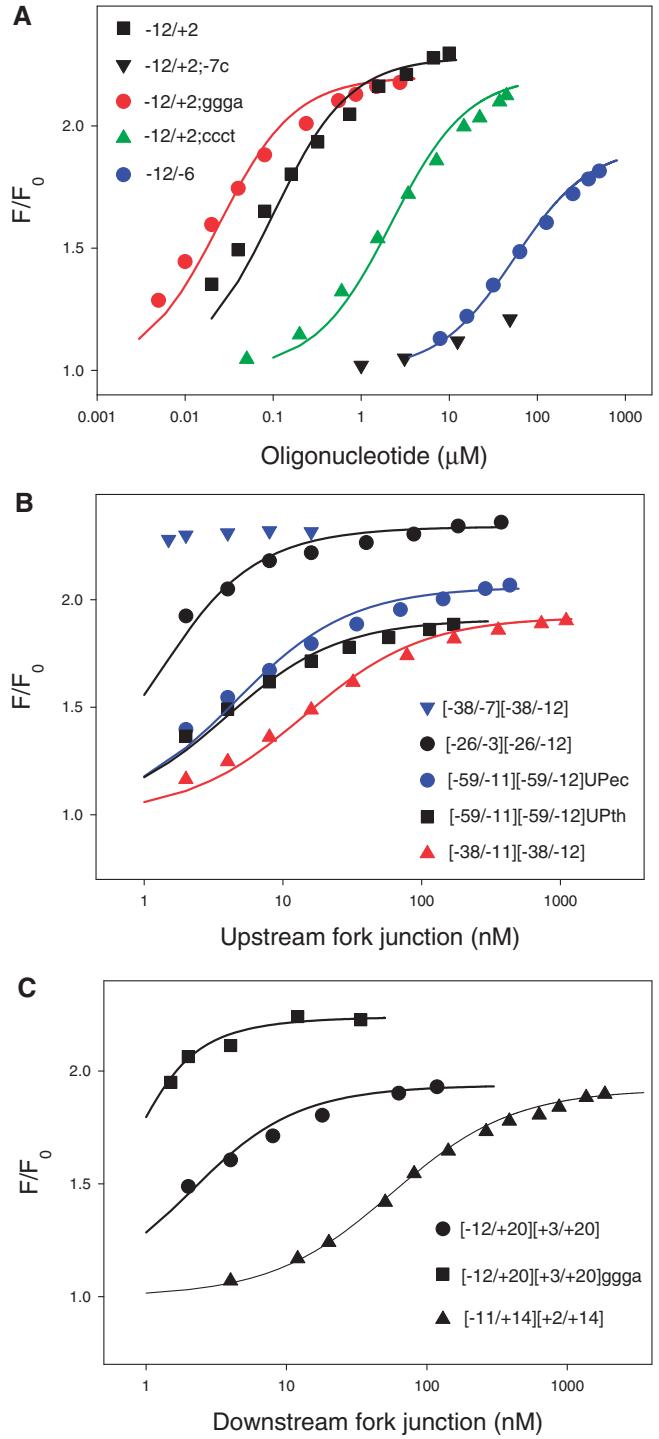


**Figure 4.** Binding of promoter fragments to *T. aquaticus* RNAP beacon. Titration of *Taq* $E\sigma^A$ beacon with oligonucleotides (**A**) or upstream (**B**) and downstream (**C**) fork junction probes is shown. Solid lines correspond to a non-linear regression fit of the data. The experimental variation of $F/F_0$ among replicate measurements usually did not exceed 15% of the average value.

The [−59/−11][−59/−12]UP*ec* and [−59/−11][−59/−12]UP*th* (probes 12 and 13) were designed to reveal additional RNAP interactions upstream of the −35 element. The sequences of these probes downstream of position −39 coincide with the [−38/−11][−38/−12] fork junction

**Table 2.** Comparison of dissociation constants for the binding of selected promoter fragments to *Taq* $E\sigma^A$ at 25°C and 45°C

| DNA probe | $K_d^{taq}$, nM | |
|---|---|---|
| | 25°C | 45°C |
| 3. −12/+2; ggga | 15 | 180 |
| 7. [−38/−11][−38/−12]TG | 1.2 | 2.6 |
| 14. [−12/+20][+3/+20] | 1.6 | 30 |
| 21. [−40/+2] | 7.1 | 3.2 |

The $K_d$ values presented are averages obtained from two to three individual experiments, the error is ±15%.

(probe 6), whereas the −39 to −59 bases represent either an optimized *E. coli* UP element sequence (probe 12) or the upstream sequence of 16 S rRNA promoter from *T. thermophilus* (33) (probe 13). As can be seen from Table 1, the affinities of probes 12 and 13 to *Taq* $E\sigma^A$ were similar and only ~4-fold higher than that of the shorter parent probe 6. In sharp contrast, *Ec* $E\sigma^{70}$ bound probes 12 and 13, respectively, 620- and 14-fold stronger, than probe 6. Thus, in agreement with previous report (14), we observe only weak non-specific interactions between upstream promoter segment and *Taq* $E\sigma^A$. In contrast, and as expected, *Ec* $E\sigma^{70}$ bound to the optimal UP element sequence much stronger than to upstream DNA present in probe 13. Higher stability of *Ec* RNAP complexes compared with *Taq* RNAP complexes is observed on promoters without UP elements (6–11) and, therefore, the upstream interactions cannot be the sole cause of higher stability of *E. coli* RNAP complexes.

### Interactions of *Taq* $E\sigma^A$ and *Ec* $E\sigma^{70}$ with downstream fork junctions

Downstream fork junctions (probes 14–16) were previously used to characterize *E. coli* RNAP promoter interactions (19). Positions of the junction points in these probes (+2 or +3) are optimal for the binding to RNAP (19) and correspond to the position of the downstream boundary of transcription bubble in $RP_o$. Therefore, RNAP interactions with the duplex segment of these downstream fork junctions likely mimic the corresponding downstream RNAP-promoter interactions in $RP_o$. A Kd value of 0.25 nM was found for *Ec* $E\sigma^{70}$ binding to [−11/+14][+2/+14] downstream fork junction (probe 16) with a relatively short duplex segment, whereas the binding to a longer [−12/+20][+3/+20] downstream fork junction (probe 14) was so strong that only a lower estimate of Kd (<0.2 nM) could be obtained (19). *Taq* RNAP affinity to probe 14 was clearly below that of *Ec* $E\sigma^{70}$ (Kd = 1.6 nM, Figure 4C, Table 1). The affinity of probe 16 to *Taq* $E\sigma^A$ was 170-fold lower than to *Ec* $E\sigma^{70}$ (Figure 4C and Table 1). The single-stranded parts of the downstream fork junctions are similar to the oligo probes, which, as shown above, bind to the *T. aquaticus* and *E. coli* RNAPs with similar affinities. Therefore, the considerably weaker binding of the downstream fork junctions to *Taq* RNAP than to the *Ec* enzyme is likely due to

weaker interaction with duplex segments located downstream of position +1.

Probes 14 and 15 differ in their sequence at positions −6/−3 (AGAT and GGGA, respectively). Comparison of Kd values for *Taq* $E\sigma^A$ binding with these probes (Kd = 1.6 and 0.2 nM, Figure 4C and Table 1) demonstrates that *Taq* $E\sigma^A$ recognizes the GGGA motif in the context of downstream fork junctions.

### Temperature dependence of *Taq* $E\sigma^A$ binding to promoter fragments

The temperature dependence of *Taq* $E\sigma^A$ and *Ec* $E\sigma^{70}$ binding to promoter DNA, upstream fork junctions and oligo templates was studied by Schroeder and deHaseth (10) using a heparin resistance assay. They found that both RNAPs bound promoter fragments better at lower temperatures, whereas the binding of DNA containing complete promoters improved when the temperature was increased (10). The downstream RNAP-promoter contacts are mainly made by RNAP domains called the lobe and the clamp, which can move relative to the central part of the enzyme (34,35). This conformational flexibility may be required for $RP_0$ formation. We considered a possibility that the low affinity of *Taq* $E\sigma^A$ to downstream fork junctions at 25°C could be improved at higher temperatures, for example, as a consequence of a conformational transition in *Taq* $E\sigma^A$ that stimulates downstream DNA binding. Accordingly, we measured Kd for *Taq* $E\sigma^A$ binding to four representative probes 1, 7, 14 and 21 (an oligo, an upstream and a downstream fork junction and a double-stranded promoter fragment without downstream DNA, correspondingly) at 45°C, a condition when the *Taq* enzyme is active, and at 25°C, when efficiency of open complex formation by $E\sigma^A$ is low (Table 2). We found that only the binding of the [−40/+2] probe was stronger at 45°C than at 25°C. The affinity of other probes dropped at higher temperature. The decreases in the oligo and downstream fork junction affinities were close (12- and 19-fold, respectively), suggesting that the temperature dependence of fork junction binding is mainly determined by its single-stranded part. The −12/+2 segment of the [−40/+2] template corresponds to the position of the transcription bubble in promoter DNA. The improvement of [−40/+2] probe affinity at higher temperature suggests that its binding to RNAP is coupled with melting of this segment, mimicking the binding of full promoter DNA. Overall, we conclude that there is no increase of intrinsically weak binding of downstream DNA to *Taq* RNAP at elevated temperatures.

### Effect of DNA downstream of the −10 element on the binding of double-stranded promoter fragments to *Taq* and *Ec* RNAPs

Previously, the strength of *Ec* $E\sigma^{70}$ beacon interaction with double-stranded DNA fragments whose downstream ends extended from −3 to +20 (probes 17–22) was measured (19). The key finding was the demonstration that a certain threshold length of downstream DNA was needed for efficient binding. We measured *Taq* $E\sigma^A$ binding to probes 17–22 to compare it with *Ec* $E\sigma^{70}$ binding. The parent probe was a [−40/+20] fragment of the T5 N25 promoter. The binding of this fragment was specific, as a control fragment bearing a C to A substitution at the critically important −11 position [−40/+20; −11 C] generated much lower signal than the wild-type probe with both enzymes (Figure 5). The binding of [−40/+20]–based probes truncated at base pairs −3, +2, +10 and +15 was assessed by measuring *Taq* $E\sigma^A$ beacon signal intensities generated by 1 nM RNAP beacon in the presence of 4 nM of each probe. The reaction temperature was 45°C. The resulting fluorescence intensities normalized to maximal signal amplitude (a signal generated by the [−40/−3] probe at a saturating concentration of 40 nM) are shown in Figure 5, along with similar data from (19) obtained with the *E. coli* RNAP beacon at 25°C. Both *Taq* and *E. coli* RNAPs generated the highest and lowest signals on the binding to [−40/−3] and [−40/+10] probes, respectively, whereas complexes with [−40/+2] generated intermediate signal amplitudes. Signals caused by the *E. coli* beacon binding to probes extended to positions +15 and +20 were close to the signal obtained with the [−40/+2] probe. In contrast, signals resulting from *Taq* $E\sigma^A$ beacon interactions with [−40/+15] and [−40/+20] were considerably lower than that observed with [40/+2]. This result suggests that *Taq* $E\sigma^A$ interactions with downstream segments of [−40/+15] and [−40/+20] are weaker than the corresponding interactions with *Ec* $E\sigma^{70}$, in agreement with the data obtained with downstream fork junctions.

### Interaction of *E. coli* and *Taq* core RNAP enzymes with DNA

*E. coli* RNAP core forms tight, slowly dissociating non-promoter complexes with DNA *in vitro* (36). Formation of such long-lived complexes of RNAP core with DNA can affect transcription from promoters and

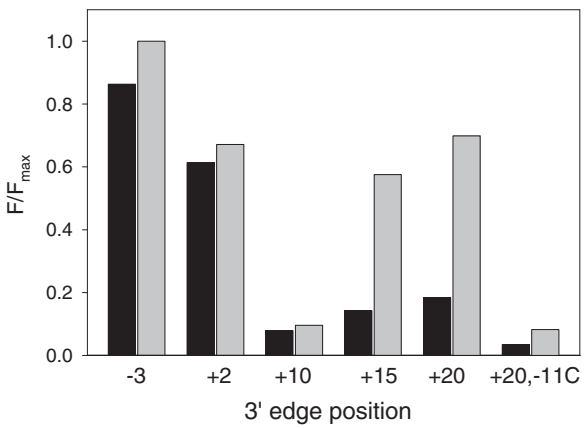


**Figure 5.** Measuring RNAP interaction with double-stranded promoter fragments using RNAP beacon assay. Normalized beacon signal amplitudes were measured in samples containing 1 nM *Taq* $E\sigma^A$ (dark bars) or *Ec* $E\sigma^{70}$ (light bars) beacons and probes truncated at the indicated positions; the probe concentrations and temperatures were 4 nM, 45°C and 2 nM, 25°C in the experiments with *Taq* $E\sigma^A$ and *Ec* $E\sigma^{70}$, respectively. The experimental variation of $F/F_{max}$ among replicate measurements did not exceed 20% of the average value.

likely should be somehow prevented *in vivo* (37). Although the structure of these non-specific complexes is unknown, the weakness of *Taq* core RNAP-mediated contacts with the downstream and upstream promoter segments in the context of *Taq* $E\sigma^A$ suggests that *Taq* core RNAP may not form stable complexes with DNA as observed for *E. coli* core RNAP. A filter-binding assay for *Taq* and *E. coli* core RNAPs interactions with N25cons promoter DNA fragment supports this suggestion (Supplementary Figure S3).

We further evaluated the inhibition effect exerted by the RNAP core interactions with DNA on the formation of *Taq* and *E. coli* RNAP holoenzymes using the beacon assay. The −10 element-containing oligos bind to *Ec* $E\sigma^{70}$ and *Taq* $E\sigma^A$ >100-fold stronger than to isolated σ subunits (18). Therefore, the kinetics of *Taq* and *E. coli* core RNAP binding to corresponding labeled σ subunits was measured by detecting the beacon signal increase caused by the addition of RNAP core to a sample containing a σ subunit and oligo probe −12/+2. Maximal signal intensities were reached in about 1 min [Supplementary Figure S4A and B, curves '($\sigma^A$ + oligo) + *Taq* core' and '($\sigma^{70}$ + oligo) + *Ec* core']. The kinetics of fluorescence intensity increase was apparently determined by the kinetics of holo RNAP formation, as oligo binding to preformed holo RNAP beacons occurred considerably faster, as shown in Supplementary Figure S4B [curve '($\sigma^A$ + *Taq* core) + oligo']. Next, we performed similar experiments with a promoterless DNA fragment shown in Supplementary Figure S4C. The non-promoter DNA itself generated only negligible signals on interaction with preformed *Taq* $E\sigma^A$ and *Ec* $E\sigma^{70}$ beacons under conditions used. In these experiments, the RNAP core enzymes were pre-incubated with the non-promoter DNA for 5 min. This pre-incubation exerted only a small effect on the rate of *Taq* $E\sigma^A$ formation [Supplementary Figure S4A, compare curves '($\sigma^A$ + oligo) + *Taq* core' and '($\sigma^A$ + oligo) + (*Taq* core + DNA)'] but considerably delayed the formation of *Ec* $E\sigma^{70}$ (Supplementary Figure S4B). Overall, the data show that *Taq* core RNAP-DNA complexes are much less stable than those formed by *Ec* core RNAP.

## DISCUSSION

Quantification of RNAP binding to model promoter fragments and comparisons of the data with known properties of promoter complexes allow one to analyse the fine details of the $RP_o$ formation. Here, we systematically applied this approach to *Taq* and *E. coli* RNAP-promoter interactions using the RNAP beacon assay. The main goal was to identify RNAP-promoter contacts, which can be responsible for the relatively low stability of promoter complexes formed by *Taq* $E\sigma^A$. Consistent with a previous report (10), our data indicate that *Taq* RNAP is not compromised in terms of its intrinsic affinity to the single-stranded non-template segment of transcription bubble bearing the −10 element. However, in agreement with the known biochemical results (32), we found that the dependence of RNAP affinity on the sequence of discriminator is different in *Taq* and *E. coli* RNAPs: the ratio of affinities of oligos 3 and 4 bearing, respectively, the GGGA and CCCT discriminator sequences is 150 for *Taq* $E\sigma^A$ and only 7 for to *Ec* $E\sigma^{70}$.

Our assay did not reveal noticeable differences in the strength of *Taq* $E\sigma^A$ and *Ec* $E\sigma^{70}$ binding to the TG motif of the extended −10 element, which is widespread among *Taq* and *Tth* promoters, or to an upstream fork junction bearing a short duplex segment (probe 11). The data obtained with longer fork junctions containing the −35 element (probes 5–7) indicate that the affinity of *Taq* $E\sigma^A$ to the consensus −35 element is moderately lower than that of *Ec* $E\sigma^{70}$. However, affinity of probe 10 with mutated −35 element to *Taq* $E\sigma^A$ is higher than to *Ec* $E\sigma^{70}$. This result is consistent with the observation that non-specific interactions of *Taq* $E\sigma^A$ region 4 with DNA suffice for activity of a T7 A1 promoter derivative (38).

The RNAP α subunit plays an important role in bacterial transcription regulation. In *E. coli*, interactions of two α subunits with various protein regulators and direct contacts of the α C-terminal domains (αCTD) with the upstream promoter DNA modulate the strength of RNAP-promoter interactions (39). In agreement with these data, our assay revealed that the consensus *E. coli* UP element stimulated *Ec* $E\sigma^{70}$ binding to probe 12 by >600-fold. An upstream segment of 16S rRNA *Tth* promoter bearing no significant sequence similarity to the UP element stimulated the *Ec* $E\sigma^{70}$ binding 14-fold, in the context of probe 13. However, in the context of the same probes, the UP element or the 16S rRNA *Tth* promoter segment stimulated the binding of *Taq* $E\sigma^A$ by only ~3.5-fold. Such weakness of upstream *Taq* $E\sigma^A$–promoter contacts suggests that αCTD-promoter interactions are unlikely to play an essential role in transcription regulation process in *Thermus*. Our results are consistent with the proposal that certain residues important for formation of the DNA-binding surface are not present in *Taq* αCTD, despite the overall similarity between the *Ec* αCTD and *Taq* αCTD structures (14).

Numerous studies indicate that downstream RNAP-promoter contacts, formed mostly by the β′ subunit, stabilize transcription initiation and elongation complexes formed by bacterial RNAPs and may decrease the energy barrier for promoter melting (15–17,40–45). A regulator of bacterial stringent response DksA decreases stability of $RP_o$ formed by *Ec* $E\sigma^{70}$ at the *rrnB* P1 promoter by disrupting downstream RNAP-promoter contacts (46). In the context of the transcription elongation complex, the downstream contacts participate in response of RNAP to pause and termination signals (4). An important new finding of this study is that RNAP contacts with promoter segment located downstream of the transcription start point are much weaker in *Taq* $E\sigma^A$ complexes than in complexes formed by *Ec* $E\sigma^{70}$. In the context of downstream fork junctions, the difference between the strength of *E. coli* and *Taq* RNAPs interactions with downstream DNA duplex is ~100-fold. We propose that similar difference of downstream RNAP-promoter interactions also exists in native promoter complexes formed by these RNAPs. Thus, the weakness of downstream interactions in *Taq* $E\sigma^A$

promoter complexes could be one of the major reasons of their low stability at moderate temperatures. At elevated temperatures, the stability of *Taq* $E\sigma^A$ transcription initiation complexes naturally increases owing to facilitation of promoter melting and the ability of the enzyme to withstand high temperature. The *E. coli* β′ subunit harbors an extensive β′In6 lineage-specific domain insertion (also called β′SI3 and β′GNCD) that is missing in *Taq* (47). Deletion of the β′In6 in *E. coli* results in destabilization of open complexes (15). Structural modeling suggests that this domain plays a role in stabilizing RNAP interactions with downstream DNA (48). Thus, the β′In6 domain likely contributes to the high affinity of *Ec* $E\sigma^{70}$ to downstream promoter DNA duplex. As noted earlier, a possibility of existence of species-specific differences in the strength of downstream RNAP-promoter contacts was already predicted basing on comparison of kinetic characteristics of *E. coli* and *B. subtilis* transcription complexes (4). Our work provides direct confirmation for this hypothesis.

On the whole, our data indicate that the difference in stability between *Ec* $E\sigma^{70}$ and *Taq* $E\sigma^A$ promoter complexes is in large part determined by difference in strength of contacts mediated by the RNAP core. In this regard, it is not surprising that the non-specific interaction of *Taq* core RNAP with DNA was found to be much weaker than in the case of *Ec* RNAP core. We speculate that this property of *Taq* RNAP may help prevent formation of long-lived *Taq* core RNAP-DNA complexes *in vivo*.

Future studies will allow more systematic elucidation of relationships between partial RNAP-promoter interactions and functional properties of complexes formed by RNAPs from various bacteria.

## SUPPLEMENTARY DATA

Supplementary Data are available at NAR Online: Supplementary Figures 1–4.

## FUNDING

National Institutes of Health [R01 GM64530 and R01 GM59295 to K.S.]; Molecular and Cell Biology Program grant from the Russian Academy of Sciences Presidium (to K.S.); ''Scientific and scientific-pedagogical personnel of innovative Russia 2009–2013'' [8475 to V.M.]. Funding for open access charge: ''Scientific and scientific-pedagogical personnel of innovative Russia 2009–2013'' [8475].

*Conflict of interest statement*. None declared.

## REFERENCES

1. Murakami,K.S. and Darst,S.A. (2003) Bacterial RNA polymerases: the wholo story. *Curr. Opin. Struct. Biol.*, **13**, 31–39.
2. Saecker,R.M., Record,M.T. Jr and Dehaseth,P.L. (2011) Mechanism of bacterial transcription initiation: RNA polymerase - promoter binding, isomerization to initiation-competent open complexes, and initiation of RNA synthesis. *J. Mol. Biol.*, **412**, 754–771.
3. Gross,C.A., Chan,C., Dombroski,A., Gruber,T., Sharp,M., Tupy,J. and Young,B. (1998) The functional and regulatory roles of sigma factors in transcription. *Cold Spring Harbor Symp. Quant. Biol.*, **63**, 141–155.
4. Artsimovitch,I., Svetlov,V., Anthony,L., Burgess,R.R. and Landick,R. (2000) RNA polymerases from Bacillus subtilis and Escherichia coli differ in recognition of regulatory signals in vitro. *J. Bacteriol.*, **182**, 6027–6035.
5. Meier,T., Schickor,P., Wedel,A., Cellai,L. and Heumann,H. (1995) In vitro transcription close to the melting point of DNA: analysis of Thermotoga maritima RNA polymerase-promoter complexes at 75 degrees C using chemical probes. *Nucleic Acids Res.*, **23**, 988–994.
6. Xue,Y., Hogan,B.P. and Erie,D.A. (2000) Purification and initial characterization of RNA polymerase from Thermus thermophilus. *Biochemistry*, **39**, 14356–14362.
7. Minakhin,L., Nechaev,S., Campbell,E.A. and Severinov,K. (2001) Recombinant Thermus aquaticus RNA polymerase, a new tool for structure-based analysis of transcription. *J. Bacteriol.*, **183**, 71–76.
8. Kuznedelov,K., Minakhin,L. and Severinov,K. (2003) Preparation and characterization of recombinant Thermus aquaticus RNA polymerase. *Methods Enzymol.*, **370**, 94–108.
9. Kulbachinskiy,A., Bass,I., Bogdanova,E., Goldfarb,A. and Nikiforov,V. (2004) Cold sensitivity of thermophilic and mesophilic RNA polymerases. *J. Bacteriol.*, **186**, 7818–7820.
10. Schroeder,L.A. and deHaseth,P.L. (2005) Mechanistic differences in promoter DNA melting by Thermus aquaticus and Escherichia coli RNA polymerases. *J. Biol. Chem.*, **280**, 7422–17429.
11. Miropolskaya,N., Ignatov,A., Bass,I., Zhilina,E., Pupov,D. and Kulbachinskiy,A. (2012) Distinct functions of regions 1.1 and 1.2 of RNA polymerase σ subunits from *Escherichia coli* and *Thermus aquaticus* in transcription initiation. *J. Biol. Chem.*, **287**, 23779–23789.
12. Paul,B.J., Ross,W., Gaal,T. and Gourse,R.L. (2004) rRNA transcription in *Escherichia coli*. *Annu. Rev. Genet.*, **38**, 749–770.
13. Ishikawa,S., Oshima,T., Kurokawa,T., Kusuya,Y. and Ogasawara,N. (2010) RNA polymerase trafficking in Bacillus subtilis cells. *J. Bacteriol.*, **192**, 5778–5787.
14. Wada,T., Yamazaki,T. and Kyogoku,Y. (2000) The structure and the characteristic DNA binding property of the C-terminal domain of the RNA polymerase alpha subunit from Thermus thermophilus. *J. Biol. Chem.*, **275**, 16057–16063.
15. Artsimovitch,I., Svetlov,V., Murakami,K.S. and Landick,R. (2003) Co-overexpression of Escherichia coli RNA polymerase subunits allows isolation and analysis of mutant enzymes lacking lineage-specific sequence insertions. *J. Biol. Chem.*, **278**, 12344–12355.
16. Bartlett,M.S., Gaal,T., Ross,W. and Gourse,R.L. (1998) RNA polymerase mutants that destabilize RNA polymerase-promoter complexes alter NTP-sensing by rrn P1 promoters. *J. Mol. Biol.*, **279**, 331–345.
17. Ederth,J., Artsimovitch,I., Isaksson,L.A. and Landick,R. (2002) The downstream DNA jaw of bacterial RNA polymerase facilitates both transcriptional initiation and pausing. *J. Biol.Chem.*, **277**, 37456–37463.
18. Mekler,V., Pavlova,O. and Severinov,K. (2011) The interaction of Escherichia coli RNA polymerase $\sigma^{70}$ subunit with promoter elements in the context of free $\sigma^{70}$, RNA polymerase holoenzyme, and the $\beta'$–$\sigma^{70}$ complex. *J. Biol. Chem.*, **286**, 270–279.
19. Mekler,V., Minakhin,L. and Severinov,K. (2011) A critical role of downstream RNA polymerase-promoter interactions in the formation of initiation complex. *J. Biol. Chem.*, **286**, 22600–22608.
20. Mekler,V., Minakhin,L., Sheppard,C., Wigneshweraraj,S. and Severinov,K. (2011) Molecular mechanism of transcription inhibition by phage T7 gp2 protein. *J. Mol. Biol.*, **413**, 1016–1027.
21. Feklistov,A. and Darst,S.A. (2011) Structural basis for promoter-10 element recognition by the bacterial RNA polymerase σ subunit. *Cell*, **147**, 1257–1269.

22. Kuznedelov,K., Lamour,V., Patikoglou,G., Chlenov,M., Darst,S.A. and Severinov,K. (2006) Recombinant Thermus aquaticus RNA polymerase for structural studies. *J. Mol. Biol.*, **359**, 110–121.
23. Sevostyanova,A., Djordjevic,M., Kuznedelov,K., Naryshkina,T., Gelfand,M.S., Severinov,K. and Minakhin,L. (2007) Temporal regulation of viral transcription during development of Thermus thermophilus bacteriophage phiYS40. *J. Mol. Biol.*, **366**, 420–435.
24. Mekler,V., Kortkhonjia,E., Mukhopadhyay,J., Knight,J., Revyakin,A., Kapanidis,A.N., Niu,W., Ebright,Y.W., Levy,R. and Ebright,R.H. (2002) Structural organization of bacterial RNA polymerase holoenzyme and the RNA polymerase promoter open complex. *Cell*, **108**, 599–614.
25. Campbell,E.A., Muzzin,O., Chlenov., Sun,J.L., Olson,C.A., Weinman,O., Trester-Zedlitz,M.L. and Darst,S.A. (2002) Structure of the bacterial RNA polymerase promoter specificity sigma subunit. *Mol. Cell*, **9**, 527–539.
26. Marr,M.T. and Roberts,J.W. (1997) Promoter recognition as measured by binding of polymerase to nontemplate strand oligonucleotide. *Science*, **276**, 1258–1260.
27. Guo,J. and Gralla,J.D. (1998) Promoter opening via a DNA fork junction binding activity. *Proc. Natl Acad. Sci. USA*, **95**, 11655–11660.
28. Heyduk,E. and Heyduk,T. (2002) Conformation of fork junction DNA in a complex with Escherichia coli RNA polymerase. *Biochemistry*, **41**, 2876–2883.
29. Tsujikawa,L., Tsodikov,O.V. and deHaseth,P.L. (2002) Interaction of RNA polymerase with forked DNA: evidence for two kinetically significant intermediates on the pathway to the final complex. *Proc. Natl Acad. Sci. USA*, **99**, 3493–3498.
30. Haugen,S.P., Berkmen,M.B., Ross,W., Gaal,T., Ward,C. and Gourse,R.L. (2006) rRNA promoter regulation by nonoptimal binding of sigma region 1.2: an additional recognition element for RNA polymerase. *Cell*, **16**, 1069–1082.
31. Feklistov,V., Barinova,N., Sevostyanova,A., Heyduk,E., Bass,I., Vvedenskaya,I., Kuznedelov,K., Merkiene,E., Stavrovskaya,E., Klimasauskas,S. *et al.* (2006) A basal promoter element recognized by free RNA polymerase sigma subunit determines promoter recognition by RNA polymerase holoenzyme. *Mol. Cell*, **23**, 97–107.
32. Barinova,N., Kuznedelov,K., Severinov,K. and Kulbachinskiy,A. (2008) Structural modules of RNA polymerase required for transcription from promoters containing downstream basal promoter element GGGA. *J. Biol. Chem.*, **283**, 22482–22489.
33. Hartmann,R.K. and Erdmann,V.A. (1989) Thermus thermophilus 16S rRNA is transcribed from an isolated transcription unit. *J. Bacteriol.*, **171**, 2933–2941.
34. Darst,S.A., Opalka,N., Chacon,P., Polyakov,A., Richter,C., Zhang,G. and Wriggers,W. (2002) Conformational flexibility of bacterial RNA polymerase. *Proc. Natl Acad. Sci. USA*, **99**, 4296–4301.
35. Chakraborty,A., Wang,D., Ebright,Y.W., Korlann,Y., Kortkhonjia,E., Kim,T., Chowdhury,S., Wigneshweraraj,S., Irschik,H., Jansen,R. *et al.* (2012) Opening and closing of the bacterial RNA polymerase clamp. *Science*, **337**, 591–595.
36. deHaseth,P.L., Lohman,T.M., Burgess,R.R. and Record,M.T. Jr (1978) Nonspecific interactions of Escherichia coli RNA polymerase with native and denatured DNA: differences in the binding behavior of core and holoenzyme. *Biochemistry*, **17**, 1612–1622.
37. Shaw,G., Gan,J., Zhou,Y.N., Zhi,H., Subburaman,P., Zhang,R., Joachimiak,A., Jin,D.J. and Ji,X. (2008) Structure of RapA, a Swi2/Snf2protein that recycles RNApolymerase during transcription. *Structure*, **16**, 1417–1427.
38. Yuzenkova,Y., Tadigotla,V.R., Severinov,K. and Zenkin,N. (2011) A new basal promoter element recognized by RNA polymerase core enzyme. *EMBO J.*, **30**, 3766–3775.
39. Lee,D.J., Minchin,S.D. and Busby,S.J. (2012) Activating Transcription in Bacteria. *Annu. Rev. Microbiol.*, **66**, 125–152.
40. Nudler,E., Avetissova,E., Markovtsov,V. and Goldfarb,A. (1996) Transcription processivity: protein-DNA interactions holding together the elongation complex. *Science*, **273**, 211–217.
41. Naryshkin,N., Revyakin,A., Kim,Y., Mekler,V. and Ebright,R.H. (2000) Structural organization of the RNA polymerase-promoter open complex. *Cell*, **101**, 601–611.
42. Korzheva,N., Mustaev,A., Kozlov,M., Malhotra,A., Nikiforov,V., Goldfarb,A. and Darst,S.A. (2000) A structural model of transcription elongation. *Science*, **289**, 619–625.
43. Vassylyev,D.G., Sekine,S., Laptenko,O., Lee,J., Vassylyeva,M.N., Borukhov,S. and Yokoyama,S. (2002) Crystal structure of a bacterial RNA polymerase holoenzyme at 2.6 A resolution. *Nature*, **417**, 712–719.
44. Saecker,R.M., Tsodikov,O.V., McQuade,K.L., Schlax,P.E. Jr, Capp,M.W. and Record,M.T. Jr (2002) Kinetic studies and structural models of the association of E. coli sigma(70) RNA polymerase with the lambdaP(R) promoter: large scale conformational changes in forming the kinetically significant intermediates. *J. Mol. Biol.*, **319**, 649–671.
45. Vassylyev,D.G., Vassylyeva,M.N., Perederina,A., Tahirov,T.H. and Artsimovitch,I. (2007) Structural basis for transcription elongation by bacterial RNA polymerase. *Nature*, **448**, 157–162.
46. Rutherford,S.T., Villers,C.L., Lee,J.H., Ross,W. and Gourse,R.L. (2009) Allosteric control of Escherichia coli rRNA promoter complexes by DksA. *Genes Dev.*, **23**, 236–248.
47. Lane,W.J. and Darst,S.A. (2010) Molecular evolution of multisubunit RNA polymerases: sequence analysis. *J. Mol. Biol.*, **395**, 671–685.
48. Chlenov,M., Masuda,S., Murakami,K.S., Nikiforov,V., Darst,S.A. and Mustaev,A. (2005) Structure and function of lineage-specific sequence insertions in the bacterial RNA polymerase beta' subunit. *J. Mol. Biol.*, **353**, 138–154.